Self assembly and correlated properties of electrospun carbon nanofibers

S.L. Rutledge [a], H.C. Shaw [a], J.B. Benavides [a], L.L. Yowell [b], Q. Chen [c], B.W. Jacobs [c],
S.P. Song [c], V.M. Ayres [c],*

[a] NASA Goddard Space Flight Center, Greenbelt, MD 20771, USA
[b] NASA Johnson Space Center, Houston, TX 77058, USA
[c] Department of Electrical and Computer Engineering, Michigan State University, East Lansing, MI 48824, USA

Abstract

An investigation of the influence of droplet size conditions and monomer choice on electrospun carbon nanofiber properties is presented. Monomer choices included poly (ε-caprolactone) and poly (methyl methacrylate) with and without the addition of single walled carbon nanotubes. A key property under investigation is the effect of electrospinning conditions on the resulting carbon nanofiber elasticity. Carbon nanofiber elasticity investigations are performed using atomic force microscopy with force volume imaging and the Force Integration to Equal Limits mapping method. A monomer choice of poly (ε-caprolactone) with a syringe bore radius of 406.4 microns is shown to produce electrospun carbon nanofibers with acceptable morphologies for tissue scaffold applications.
© 2006 Elsevier B.V. All rights reserved.

1. Introduction

Electrospun carbon nanofibers are hollow core carbon structures produced by self-assembly within an evaporating liquid jet. They are of great interest as biocompatible carbon-based structures for tissue scaffold applications [1].

Electrospinning-based self-assembly is achieved by the application of an electrostatic force between a charged droplet containing polymer monomers in liquid suspension and a collecting metal electrode [2–4]. A charged droplet of monomer in liquid suspension is formed at a capillary tip, conveniently a metal syringe tip of known bore radius. A 20–30 kV potential difference is applied between the syringe tip and a metal collecting plate held 10–20 cm apart. At a critical field, the force due to the electric field overcomes the surface tension forces holding the droplet, and the solution starts flowing towards the collecting electrode in the form of a charged jet. Initially, the charged droplet deforms into a cone, which then separates into splayed charged jets due to mutual repulsion. As the liquid in each splayed jet evaporates, the jet diameter shrinks rapidly, creating the conditions for self assembly of the polymers into nanofibers. The diameters of the collected electrospun carbon nanofibers may range from a few microns to as low as 10 nm depending on the complicated interplay of Coulomb forces. Electrospun carbon nanofibers used in tissue scaffold applications typically have diameters on the order of ∼ 100 nm.

In this work, results of an investigation of monomer choice, to control the initial droplet charge state, and syringe bore size, to control the initial droplet radius/surface tension, are presented. In Series 1, 15% weight of poly methyl methacrylate suspended in tetrahydrofuran (THF)/dimethylformamide (DMF) was electrospun using a 200 μm fixed bore radius, without and with the addition of 6% single walled carbon nanotubes produced by NASA-GSFC Cooled Welding Method added to the suspension. In Series 2, 15% weight of poly (ε-caprolactone) suspended in methylene chloride (MC)/dimethyl-formamide (DMF) was electrospun using bore radii of 152.4, 254.0 and 406.4 μm. The tip to collector plate distance was held constant at 10 cm. The voltage was held constant at 25 kV. A key property under investigation in our group is the effect of electrospinning conditions on resulting carbon nanofiber

elasticity. Recent research indicates that the elasticity of the tissue scaffold is an important property for successful entrained cell re-growth. The Force Integration to Equal Limits (FIEL) mapping method [5,6] was used to measure the relative elasticity between the samples.

2. Experimental methods

2.1. Experimental

Poly(methyl methacrylate) (PMMA) with a molecular weight of 120,000 and poly (ε-caprolactone) with a number average molecular weight (M_n) of 80,000 from Aldrich Chemical were used in these experiments (Fig. 1a–b). Single walled carbon nanotubes, 6% by weight, produced by NASA-GSFC Cooled Welding Method were added to one batch of PMMA experiments. The electrospinning set-up consisted of a Sorensen 230-3/12P R&D high voltage DC power supply, with a syringe and an $8 \times 12''$ aluminum collecting foil held 10 cm apart. The experiments were horizontally configured, with the syringe tilted about 30° to facilitate droplet formation (Fig. 1c). Field emission scanning electron microscopy (FESEM) of gold coated samples was used to assess the initial non-woven mat topography and nanofiber diameter, and to confirm that subsequent atomic force microscopy results were truly representative. Field emission scanning electron microscopy was performed using a Hitachi S-4700II Field Emission SEM operated at 1.0 kV.

Atomic force microscopy (AFM) with force volume imaging [7] was performed using a Veeco Metrology Nanoscope IIIa Scanning Probe Station, in contact mode with a nominal tip radius of 25 nm, operated in ambient air. A silicon nitride tip was used. The silicon nitride tip (hardness ≈ 35 GPa) was assumed to be much harder than any of the tissues scaffold samples.

2.2. FIEL mapping method for relative elasticity

In force volume imaging, a single force curve records the force felt by the tip as it approaches to and retracts from a point on the sample surface. A force volume image consists of an array of force curves over a user-specified area. Each force curve is measured at a unique $X–Y$ position within the area and force curves from an array of $X–Y$ points are combined into a three dimensional array of force data.

The Force Integration to Equal Limits (FIEL) mapping method can be used to produce a robust measurement of relative elasticity between samples. In FIEL mapping, force curves (FC) taken during force volume imaging are used to measure the cantilever deflection (d) versus the sample position (Z). The FCs are taken in Relative Trigger mode, in which the sample is advanced until a preset cantilever deflection relative to the zero deflection position is reached, as measured by the AFM optical detection system A corresponding Force Distance (FD) curve is defined by using an absolute distance ($D=Z-d$), which is the separation between the tip and the sample surface, instead of using sample position (Z). If the AFM tip is approximated as a parabola with a spherical tip (Hertz model), then the force on the AFM cantilever (F) can be calculated by

$$F = \frac{4E\sqrt{R}}{3(1-v)}\delta^{3/2} \tag{1}$$

where E is the elastic modulus of the sample, R is the radius of the probe sphere, δ is the indentation and v is the Poisson ratio. The relationship between elasticity and FD curves derived from FIEL mapping method is

$$w = \int_0^{\delta_{max}} Fd\delta = \int_0^{\delta_{max}} \frac{4}{3}\frac{\sqrt{R}}{\pi k}\delta^{3/2}d\delta$$
$$= \frac{8}{15}\frac{\sqrt{R}}{\pi k}\delta_{max}^{5/2} \text{ (N m)} \tag{2}$$

where

$$k = \frac{1-v}{\pi E} \tag{3}$$

is the local elastic constant, and w is the work done by the cantilever, which is equal to the area under the FD curve. The area under the FD curve (w) can then be graphically calculated and used to represent the elasticity feature of the tissue scaffolding.
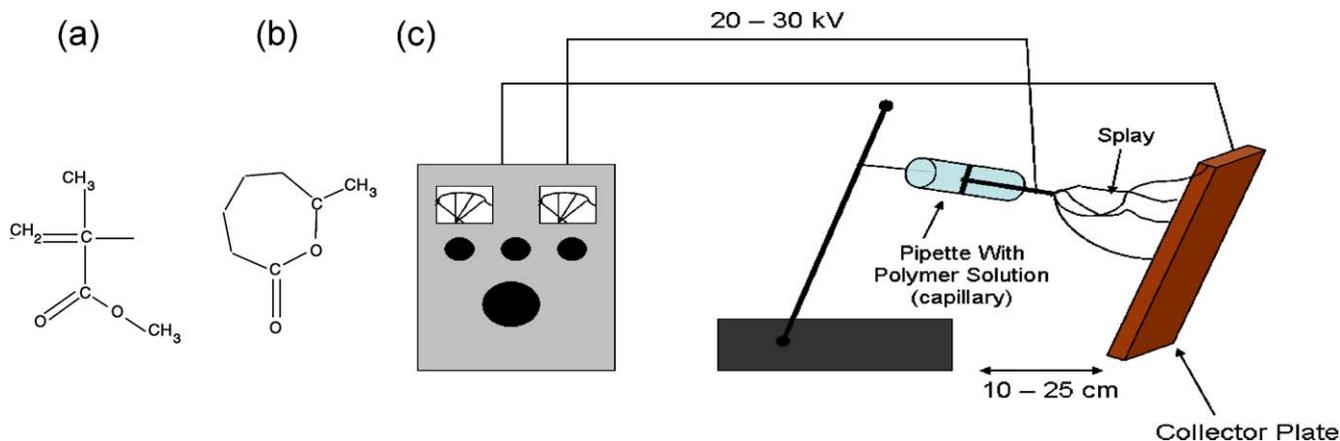

Fig. 1. Polymer monomers (a) poly (methyl methacrylate), and (b) poly (ε-caprolactone). (c) Experimental configuration of electrospinning experiment.
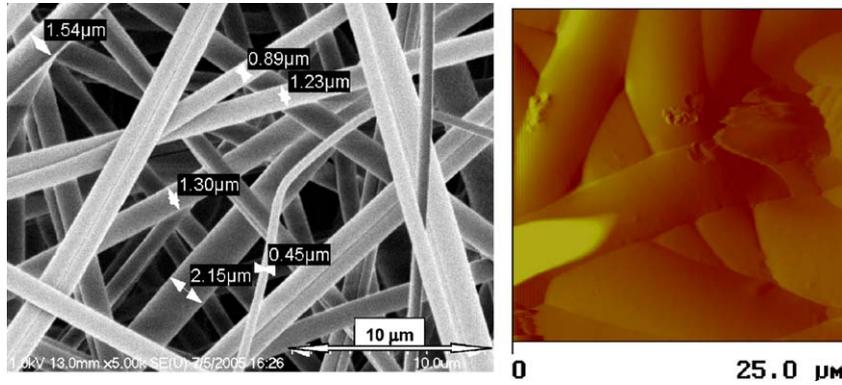
Fig. 2. (a) Field emission SEM of PMMA-based carbon nanofibers and (b) atomic force microscopy of PMMA-based carbon nanofibers with 6% weight of single walled carbon nanotubes added. A 200-μm bore radius resulted in micron-scale diameter nanofibers.

The FIEL mapping method may be used to define the relative elasticity of the different samples as follows. Using the method of Ref. [5], the FD curves must be acquired using the same tip/cantilever. The tip should be much harder than the sample. The elastic properties of the sample are assumed to dominate any viscous properties and plasticity is not considered. Under these conditions, the externally applied force of Eq. (1) may be assumed to be the same and what changes is the elastic response of the sample. Using Eqs. (1)–(3) and graphically evaluating the relative work as the areas under two FD curves,

$$\frac{w_1}{w_2} = \left(\frac{k_1}{k_2}\right)^{2/3} \qquad (4)$$

which directly relates the areas under two FD curves to the ratio of their elastic constants. The relative sample elasticity is given by the inverse power relationship of Eq. (3).

3. Results

The PMMA monomers with and without single walled carbon nanotubes were electrospun under conditions of 200 μm bore radius, 10 cm between the tip and the collector foil, and 25 kV electrostatic potential difference. The results are shown in Fig. 2. Electrospinning of both resulted in micron-scale diameter fibers. This is too large for tissue scaffold applications and PMMA was not investigated further. Anomalous beam and tip deflections observed during the electron and atomic force microscopy experiments indicated highly charged surface states.

The poly (ε-caprolactone) monomers were electrospun under conditions of 10 cm between the tip and the collector foil and 25 kV electrostatic potential difference. The bore radius was varied through (a) 152.4, (b) 254.0, and (c) 406.4 μm. The results are shown in Fig. 3.
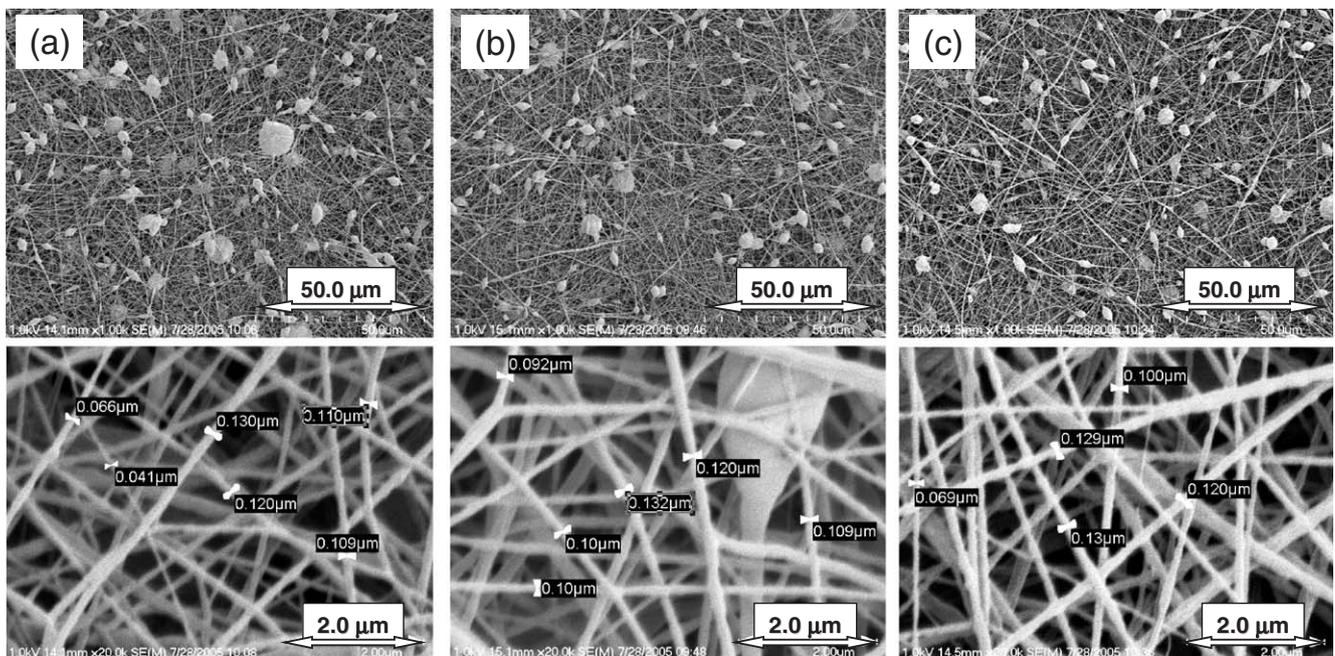

Fig. 3. Field emission SEM of poly (ε-caprolactone) carbon nanofibers spun at bore radii (a) 152.4, (b) 254.0, and (c) 406.4 μm. As the bore size was increased, a slight increase in fiber diameter with a large decrease in bubble size was observed.

The nanofiber average diameter was ~90–110 nm, increasing slightly as the bore size was increased. Nuisance bubbles were observed in addition to the nanofibers. The average diameter of the nuisance bubbles deceased by ~50% as the bore size was increased.

Atomic force microscopy with force volume imaging followed by Force Integration to Equal Limits (FIEL) mapping was used to measure the relative elasticity between the three poly (ε-caprolactone) nanofiber samples and the metal foil. The results of the FIEL elasticity mapping for the poly (ε-caprolactone) samples are shown in Figs. 4 and 5. A 5 μm² region of each sample (Fig. 4, left) was selected for analysis to ensure that a statistically meaningful number of force curves were taken on several nanofibers. As the AFM tip is vertically indenting a cylindrical object, only data collected along the top and center of each nanofiber matches the model. An erosion operation [6,8] was performed along each nanofiber to restrict the data set to these reliable points. The area under each force distance curve was plotted as a map along each nanofiber. A typical result for the topmost nanofibers is shown in Fig. 4 (middle). A histogram of the values shown in Fig. 4 (right) indicated that there were differences in the value distributions among the samples. The values of the areas under the force distance curves increased with increased bore radius. The result shown in Fig. 5 is the mean value for data similarly analyzed along several nanofibers. The mean value force distance curve areas increased with increased bore radius as shown in the Fig. 5 insets. As the area (w) is in an inverse power relationship with the elasticity E as shown in Eqs. (3) and (4), these results indicate a decrease in sample elasticity (E) with increasing bore radius.

4. Discussion and conclusion

A 15% weight of poly (ε-caprolactone) suspended in methylene chloride (MC)/dimethylformamide (DMF) was shown to produce electrospun carbon nanofibers with average diameters ~90–110 nm. The average nanofiber diameter was observed to increase slightly as the bore size was increased. There is a large body of research on control of electrospun nanofiber diameter, which indicates that the monomer charge density and polymer solution concentration have the greatest influence, by varying the charge concentrations, and hence the Coulomb forces [2–4]. For electrospun carbon nanofibers used
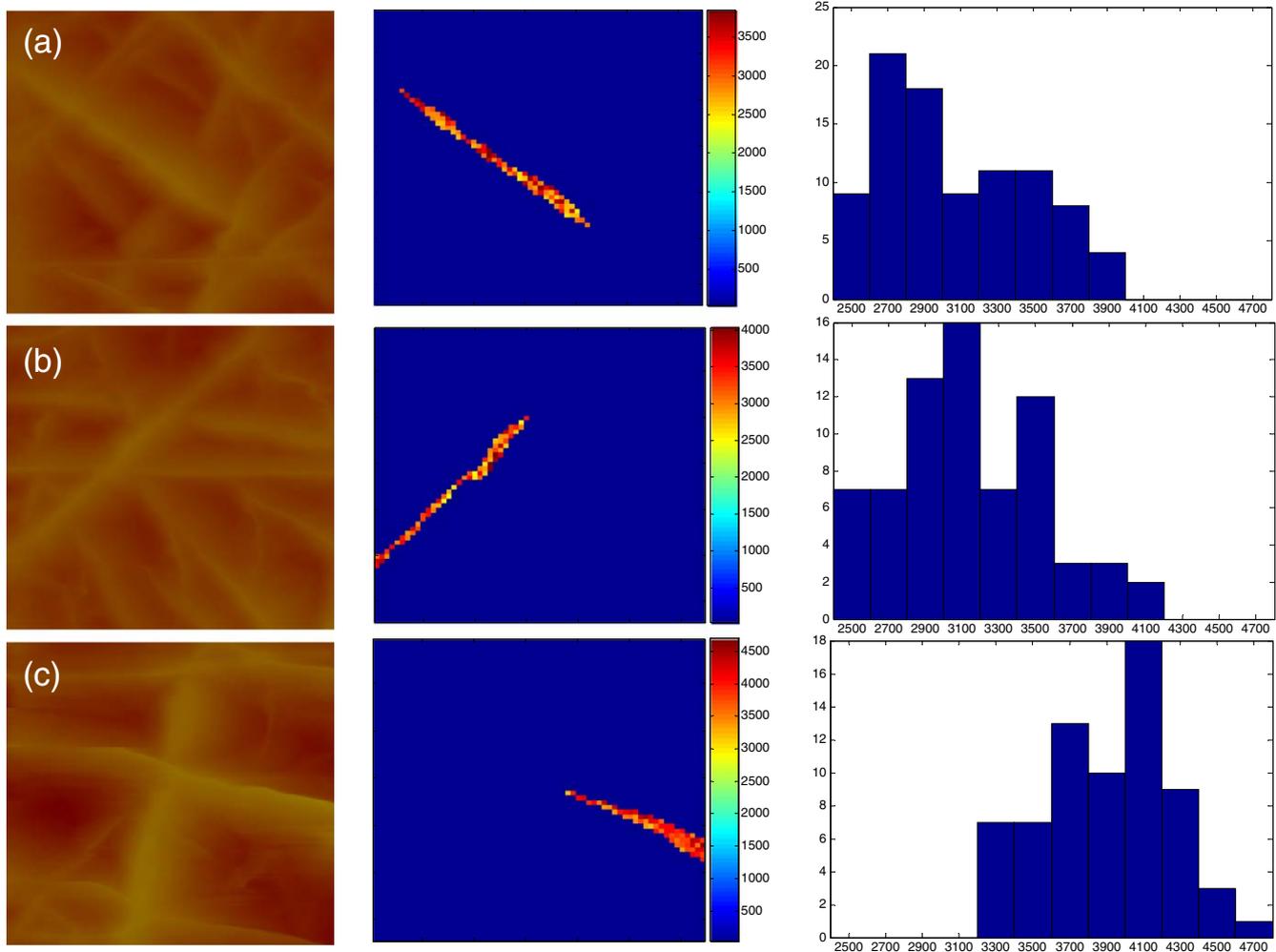

Fig. 4. Atomic force microscopy (left) and Force Integration to Equal Limits elasticity maps (middle) of relative elasticity for poly (ε-caprolactone) nanofibers spun at bore radii (a) 152.4, (b) 254.0, and (c) 406.4 μm. Histograms (right) of the values show different distributions between the samples.
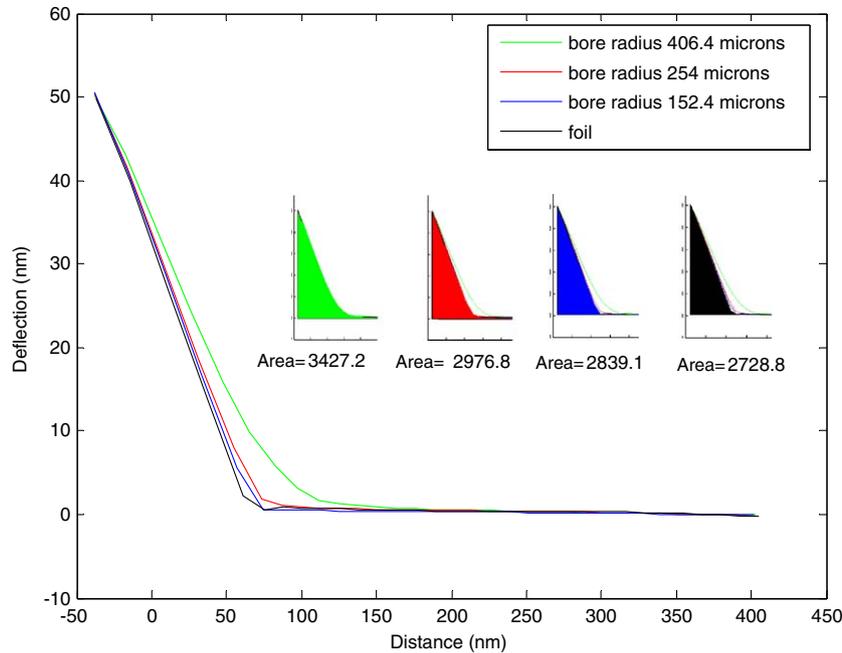
Fig. 5. Mean value force distance curves from data analyzed along several nanofibers and the aluminum foil. The mean value force distance curve areas increased with increasing bore radius (insets), indicating a decrease in nanofiber elasticity (E) with increasing bore radius.

in tissue scaffold applications, diameters that mimic the structural portion of the extracellular matrix (ECM) are desirable. The ECM is composed of fibrillar collagen 50–300 nm in diameter. Therefore, the Series 2 nanofibers had acceptable diameters for potential tissues scaffold applications.

Recent research indicates that the elasticity of the tissue scaffold is another important property for successful entrained cell re-growth [9,10]. In this work, the FIEL mapping method was used for the first time to relate variations in electrospinning conditions to relative elasticities among candidate scaffolds. The scaffolds with a known relative elasticity sequence will now be tested for entrained cell growth for various types of cells, and the results reported in a future publication. The AFM-based FIEL mapping method [5] applied to reliable data points [6] along individual ∼ 100 nm diameter nanofibers is a powerful technique to determine the relative elasticity sequence.

The mean value force distance curves for data analyzed along several nanofibers indicated a decrease in relative elasticity with increasing bore radius. This is a new result. Increasing the bore radius increases the diameter and therefore the surface tension of the initial spherical monomer-containing droplet. The correlations between this and the applied field conditions leading to the onset of cone deformation followed by charged single jet production, and their influence on nanofiber self-assembly conditions, are currently under investigation by our group.

Acknowledgements

References

[1] A. Plant, A. Chilkoti, A.E. Barron, J. Wong (Eds.), Architecture and Applications of Biomaterials and Biomolecular Materials, The Materials Research Society, Warrendale, PA, 2004.

[2] B. Sundaray, V. Subramanian, T.S. Natarajan, R.-Z. Xiang, C.-C. Chang, W.-S. Fann, Appl. Phys. Lett. 84 (2004) 1222.

[3] K.H. Lee, H.Y. Kim, M.S. Khil, Y.M. Ra, D.R. Lee, Polymer 44 (2003) 1287.

[4] J.R. Lee, S.J. Park, M.K. Seo, J.M. Park, in: Mircea Chipara, David L. Edwards, Roberto S. Benson, Shawn Phillips (Eds.), Materials for Space Applications, Mater. Res. Soc. Symp. Proc., vol. 851, NN 5.11, The Materials Research Society, Warrendale, PA, 2005.

[5] E. A-Hassan, W.F. Heinz, M.D. Antonik, N.P. D'Costa, S. Nagaswaran, C.A. Schoenenberger, J.H. Hoh, Biophys. J. 74 (1998) 1564.

[6] Q. Chen, Y. Fan, V.M. Ayres, L. Udpa, M.S. Schindler, A.F. Rice, in: S.V. Kalinin, B. Goldberg, L.M. Eng, B.D. Huey (Eds.), Scanning-Probe and Other Novel Microscopies of Local Phenomena in Nanostructured Materials, Mater. Res. Soc. Symp. Proc., vol. 838E, O15.2, The Materials Research Society, Warrendale, PA, 2005.

[7] Veeco Metrology Group Support Note 228, Rev. E, Force Imaging.

[8] R.C. Gonzales, R.E. Woods, Digital Image Processing, Addison-Wesley, Boston, MA, 1993.

[9] H.G. Doebereiner, B.J. Dubin-Thaler, G. Giannone, H. Xenius, M.P. Sheetz, Bull. Am. Phys. Soc. 49 (1) (2004) B8.7.

[10] C.M. Lo, H.B. Wang, M. Dembo, Y.L. Wang, Biophys. J. 79 (2000) 144.